This is a repository copy of *Preparation and properties of UV-curable hyperbranched polyurethane acrylate hard coatings*.

Preparation and Properties of UV-curable Hyperbranched Polyurethane Acrylate Hard Coatings

aJunchao Fu, aHaojie Yu*, aLi Wang*, bLong Lin, aRizwan Ullah Khan.

a State Key Laboratory of Chemical Engineering, College of Chemical and Biochemical Engineering, Zhejiang University, Hangzhou 310027, China

b Department of Colour Science, University of Leeds, Woodhouse Lane, LS2 9JT, Leeds, UK

_____

Abstract: In order to efficiently protect plastic cover of 5G mobile phones, a novel hyperbranched polyurethane acrylate-based hard coating (HBPUA) having highly rigid hyperbranched cores was prepared and used as the protective film. For purpose of researching the structure and property relationship, two more hyperbranched cores (Hyper-6OH) and corresponding HBPUA oligomers were also synthesized. The structures of Hyper-6OH and HBPUA were characterised by proton nuclear magnetic resonance, and the molecule weight of HBPUA was confirmed by gel permeation chromatography. To further enhance the crosslinking and lower the internal stress, pentaerythritol tetra(3-mercaptopropionate) (PETMP) was introduced into the film system. The curing behaviours of the prepared HBPUA coatings were determined by Fourier-transform infrared spectroscopy. The results indicated that the double bond conversion was associated with the rigidity of the hyperbranched core and the content of thiol groups. The properties of HBPUA-based films were characterized by the test of gel content, swelling ratio and water absorption and as well as dynamic mechanical property, mechanical property, thermogravimetry and surface property. The results reveal that the pencil hardness of the prepared coatings reaches 5H that is higher than the commercially available resin PUA-6, enabling potential application in the protection of plastic cover.

The rigidity of the hyperbranched cores and the introduction of PETMP remarkably affect the T_g

value of the films, and the addition of thiol groups increases the gel content, swelling ratio,

toughness and adhesion of coatings, but decreases the water absorption and tensile strength.

Moreover, all coatings exhibit good thermal properties.

_____

* Correspondence to Prof. Haojie Yu, E-mail: hjyu@zju.edu.cn and Li Wang, E-mail: opl_wl@dial.zju.edu.cn. Tel: +86-571-8795-3200; Fax: +86-571-8795-1612.

1. Introduction

Polycarbonate (PC) has been used to fabricate covers for 5G mobile phones. However, PC plastic

surface possesses inferior hardness, which limits its application[1-4]. Hence, there exists a desire to

improve the surface hardness of PC plastic, without compromising its other mechanical properties.

Among all potential technical solutions, using the hard coating to protect the plastic surface is a

widely used strategy because of its low cost, convenience and facile process[5].

As a kind of widely used UV-curable resin, polyurethane acrylate (PUA) possesses an excellent

photo-reactivity, abrasive resistance and a series of adjustable features[6-9]. Nevertheless, due to the

inadequate content of photosensitive groups within PUA, it is difficult to create hard films using

general purpose PUA via dense network structure. In recent years, several strategies that are

advantageous for enhancing the film hardness have been reported. Thus, _Li et al._[10] introduced

pentaerythritol triacrylate (PETTA) as a reactive diluent into the base resin, and found that the pencil

hardness of coatings was raised from 2H to 3H with the increment of the content of PETTA due to

the increased crosslinking afforded by the poly-functionality of PETTA. _Park et al._[11] illustrated that

1   the compact network structure formed by the addition of vinyltrimethoxysilane coupling agents

2   could account for the increased hardness. *Mishra et al.*[12] synthesized an intermediate named dimer

3   acid modified epoxy polyol, which was incorporated into PUA chains, revealing that the rigidity of

4   phenyl groups could remarkably enhance the hardness of coatings. *Zhang et al.*[13] obtained an

5   organic-inorganic hybrid material through introducing aqueous colloidal silica into PUA matrix.

6   Owing to the nanometric effect, the film hardness was improved from 2H to 5H, but the uneven

7   surface on the resultant coating was observed because of the aggregation of particles. *Liu et al.*[14]

8   used renewable cardanol as polyols to prepare hyperbranched UV-curable oligomers, which not only

9   reduced the viscosity of resins but also increased the content of acrylate groups, subsequently

10   significantly enhancing the coating hardness from HB to 3H. Although the promotion of the coating

11   hardness in the above-mentioned methods was achieved, certain disadvantages were introduced by

12   the insufficient content of photosensitive groups of the base resin resulting in the low crosslink

13   density, or the incorporation of phenyl groups leading to the yellowing of resultant coatings, or the

14   introduction of inorganic nanoparticles resulting in the rough film surface[15].

15   Due to the application field of hard coatings being for PC plastic cover, such characteristics of the

16   film-forming resin as low viscosity and abundant photosensitive groups of the resin, anti-yellowing

17   and smooth surface of the resultant coating should be borne in mind. Hence, the alicyclic

18   hyperbranched polyurethane acrylate oligomer is preferred as the base resin due to its low viscosity,

19   plentiful terminal acrylate groups and absence of benzene ring, especially combining with the rigid

20   groups resistant to yellowing which are used as the hyperbranched core.

21   In this study, the hyperbranched core (Hyper-6OH) with high rigidity and six terminal hydroxyl

22   groups was synthesized firstly by click chemistry between monothioglycerol (MTGL) and 2,4,6-

triallyloxy-1,3,5-triazine (TAC). Subsequently, the novel HBPUA oligomer was obtained via the reaction of Hyper-6OH, isophorone diisocyanate (IPDI), hydroxybutylacrylate (HBA) and trimethylolpropane diallylether (TMPDE). In order to study the effect of rigid cores on properties of resultant coatings, the other two hyperbranched cores and corresponding HBPUA oligomers were prepared. A series of UV-curable coatings were prepared by dissolving HBPUA and photoinitiators into isopropanol (IPA) to obtain homogenous solutions. For purpose of further promoting the crosslink density and reducing internal stress, PETMP was added. The commercially available resin PUA-6 was used as a benchmark against which the surface property of the compounds developed through the study reported here were compared. The properties including UV-curing behaviour, surface property as well as the dynamic mechanical property, mechanical property and thermal property of the cured films were investigated.

2. Experimental

2.1 Materials

2,4,6-triallyloxy-1,3,5-triazine (TAC), 1,3,5-triacryloylhexahydro-1,3,5-triazine (TAT), trimethylolpropane trimethacrylate (TMPTA), isophorone diisocyanate (IPDI), 4-hydroxybutylacrylate (HBA), pentaerythritol tetra(3-mercaptopropionate) (PETMP), 2-hydroxy-4'-(2-hydroxyethoxy)-2-methylpropiophenone (Irgacure 2959, as photoinitiator), dibutyltin dilaurate (DBTDL, as catalyst) and 4-methoxyphenol (MEHQ, as inhibitor) were purchased from J&K Scientific Ltd. (Beijing, China). Trimethylolpropane diallylether (TMPDE) and monothioglycerol (MTGL) were purchased from Sigma Aldrich. Irgacure 184 and Irgacure TPO were purchased from Shanghai Hound-Chase Fine Chemical Co., Ltd. The commercially available polyurethane acrylate resin 6145-100 (PUA-6, six arms) was supplied by Eternal Materials Co. Ltd. (Jiangsu, China). All

1 of the chemical reagents were used as received.

2.2 General procedure for the synthesis of TAC-MTGL

The synthesis of TAC-MTGL was conducted according to a reported strategy[16]. TAC (4.9818 g, 20.01 mmol), MTGL (6.8061 g, 63.02 mmol) and Irgacure 2959 (269.5 mg, 1.20 mmol) were added into a 50 mL beaker. The contents of the beaker were warmed up slightly to solubilise the photoinitiator Irgacure 2959, then thoroughly mixed and irradiated, without stirring, with a 365 nm light source (100 W) at ambient temperature. The reaction was conducted until the disappearance of allyl double-bond at 920 cm^{-1} in the Fourier-transform infrared spectroscopy (FTIR) spectra (around 0.5 h). The irradiated contents were subsequently dissolved in 30 mL methanol and precipitated three times into 300 mL petroleum ether/diethyl ether (V1:V2=5:1), following which a clear viscous liquid was obtained.

2.3 General procedure for the synthesis of TAT-MTGL and TMPTA-MTGL

TAT-MTGL and TMPTA-MTGL were prepared by a slightly modified method previously reported[17]. For the synthesis of TAT-MTGL, TAT (4.9806 g, 20.00 mmol), n-propylamine (44.5 mg, 0.75 mmol, as catalyst) and 20 mL methanol were introduced into a 100 mL three-necked flask. Whilst stirring, MTGL (6.8089 g, 63.05 mmol) in 10 mL methanol was added dropwise over 20 min through the air inlet at ambient temperature. The reaction was carried out until the disappearance of acrylate double-bond at 810 cm^{-1} in the FTIR spectra (about 0.5 h). Subsequently, the contents of the flask were precipitated into 300 mL petroleum ether/diethyl ether (V$_1$:V$_2$=5:1) once to obtain a crystalline, hard, white solid after vacuum drying. TMPTA-MTGL was prepared according to the same synthetic route and the same mole ratio to TAT-MTGL, and a viscous liquid was obtained after purification.

2.4 Synthesis of hyperbranched polyurethane acrylate HBPUA-TAC, HBPUA-TAT and

5

HBPUA-TMPTA

To a 100 mL three-necked flask equipped with a reflex condenser, a magnetic stirrer and a nitrogen inlet, IPDI (8.8848 g, 40.02 mmol), DBTDL (80.2 mg, 0.5 wt%), MEHQ (64.2 mg, 0.4 wt%) and 5 mL THF were added to react with TMPDE (4.2801 g, 20.00 mmol), HBA (2.8803 g, 20.00 mmol) and 10 mL THF which were introduced dropwise into the solution over 1 h. The reaction was continued at 35 °C until the -NCO group content reached the theoretical isocyanate value (about 4 h) which was determined by standard di-*n*-butylamine back titration method (ASTM D 2572)[13], and then the solution was heated to 60 °C. Then, the mixed solution of TAC-MTGL (3.7325 g, 6.51 mmol) and 10 mL DMF was added into the above-mentioned reaction vessel and stirred until -NCO group at 2274 cm^{-1} disappeared from the FTIR spectra (around 10 h)[13]. Finally, a white solid HBPUA-TAC was obtained by precipitating the content of the reaction vessel twice into 400 mL hexane/ethyl ether (V_1:V_2=4:1). The same mole ratio and reaction route were employed for the synthesis of HBPUA-TAT and HBPUA-TMPTA.

2.5 Preparation of UV-curable coatings

The HBPUA oligomers (HBPUA-TAC, HBPUA-TAT and HBPUA-TMPTA) were firstly dissolved in IPA to obtain a homogeneous system, respectively. Then, 4 wt% photoinitiators (according to polyurethane acrylate resin, the weight ratio between Irgacure 184 and Irgacure TPO was 4:1) were added to the mixture. PETMP was added into each formulation and stirred for 10 min to form a homogenous system. The PUA-6 formulation was prepared in the same way without PETMP. Detailed compositions of the UV-curing coatings are listed in **Table 1**.

A 3 cm × 3 cm polycarbonate sheet was dip-coated with the UV-curing resin. After being allowed to levelling for 1 min, the coated polycarbonate sheet was dried at 60 °C for 5 min, and then

1 irradiated with a high-pressure mercury lamp (1 kW, dose: around 800 mJ/cm^2), at a distance of 15

2 cm from the lamp, for 30 s. The thickness of the final coating was about 30 μm for coating

3 characterisations. Films with thickness about 300 μm were prepared for thermal and mechanical

4 tests by pouring the UV-curing resin into a Teflon mold to produce the film sheets following the

5 same procedure. All samples were stored in desiccator for 3 days to allow aging before

6 characterisations and tests were carried out[6,18].

7 **2.6 Characterisation**

8 Proton nuclear magnetic resonance (^{1}H NMR) analyses of the oligomers were conducted using a

9 Bruker Advanx-400 DMX NMR spectrometer at 25 °C, using DMSO-d$_6$ or CDCl$_3$ as solvent. The

10 molecular weight and molecular weight distribution (PDI) of the polyurethane acrylate oligomers

11 were measured using Water 515-2414 gel permeation chromatography (GPC), where

12 tetrahydrofuran (1.0 mL/min) was used as the mobile phase and polystyrene standards were

13 employed to determine the relative molecular weights. The conversion of double bonds and thiol

14 groups were investigated using Nicolet 5700 FTIR spectrometer (Number of scans: 130, 000 times

15 per second, wavelength range: 4000-400 cm^{-1} and resolution: 0.09 cm^{-1}) and the absorbance of the

16 samples were measured before and after UV-irradiation by a high-pressure mercury lamp with main

17 wavelength at 365 nm (BLTUV, Dongguan BLTUV Technology Co. Ltd., China). All of the samples

18 analysed by FTIR were coated on KBr disks. The viscosity of the prepared coating solution was

19 tested by HAAKE RS6000 viscometer from 1 Hz to 100 Hz at 25 °C.

20 Pencil hardness was measured according to ASTM D 3363 (The pencil hardness test was performed

21 under the load of 1kg.). Crosshatch adhesion test was performed according to ASTM D 3359. The

22 flexibility of the coatings was estimated according to GB12754. The gel content was assessed

according to ASTM D2765. The weight loss of the cured films after a 48 h extraction with acetone

was measured, and calculated by eqn. (1):

$$Gel = W_1 / W_0 \times 100 \quad (1)$$

where W_0 and W_1 are the mass of the UV-cured coatings before and after extracting in a Soxhlet

extractor. The swelling ratio and water absorption of coatings were also calculated, using following

equations:

$$Swelling = (W_2 - W_1)/ W_1 \times 100 \quad (2)$$

$$Absorption = (W_3 - W_1)/ W_1 \times 100 \quad (3)$$

where W_1 represents the coating weights after Soxhlet extraction, and W_2 and W_3 represent the

coating weights after swelling by acetone and absorbing water at room temperature for 48 h,

respectively.

Tensile strength of the film sheets was obtained using a Zwick/Roell Z020 testing machine. Thus,

dumbbell-shaped specimens (gauge length: 20 mm; width: 3 mm; thickness: 0.3 mm) were tested

at a crosshead speed of 5 mm/min at 25 °C and around 60% RH. Dynamic mechanical analysis

(DMA) was determined by a TAQ800 instrument in tensile mode with film dimensions set at 20

mm × 3 mm × 0.3 mm ($L \times W \times H$). The operating parameters were 1 Hz, 5 μm amplitude and a

heating rate of 3 °C/min from -25 to 110 °C. The thermal stability of all of the films were estimated

under nitrogen atmosphere by thermogravimetric analysis (TGA) carried out on a TA-Q500

instrument with a constant heating rate of 10 °C/min from 50 to 650 °C.

3 Results and Discussion

3.1 Preparation and characterisation of Hyper-6OH and HBPUA oligomers and synthesis routes of corresponding coatings

1　The Hyper-6OH was firstly synthesised by the facile and rapid thiol-ene 'click' reaction[19], and the

2　synthesis scheme and ^{1}H NMR spectra for Hyper-6OH are shown in **Scheme 1a** and **Figure S1**,

3　respectively. Subsequently, HBPUA oligomers were prepared through the reaction between

4　isocyanate groups and hydroxyl groups, and this reaction could be controlled by the different

5　activities of two isocyanate groups in IPDI at low reaction temperature due to the steric and

6　electronic effect[20]. In order to prevent the prepared oligomers from increasing molecular weight or

7　inducing gelation as a result of thermal polymerization of sufficient acrylate groups, the HBA

8　moiety was partially replaced by TMPDE during reaction. The synthesis scheme for HBPUA

9　oligomers is described in **Scheme 1b**. The ^{1}H NMR spectra and GPC curves of HBPUA oligomers

10　are displayed in **Figure S2** and **Figure S3**, respectively. During the process of preparing coatings,

11　as the preferred industrial coating process is dip-coating, the low viscosity of the UV-curing system

12　is essential in order to allow satisfactory levelling of the resultant coatings. Therefore, IPA was used

13　as the diluent due to its appropriate boiling point and limited impact on the PC cover. Finally,

14　coatings based on HBPUA were obtained after UV-curing. It was found that the PETMP added into

15　the UV-curable system facilitated the conversion of C=C and consequently reduced the internal

16　stress of the compact network structure[19]. Detailed recipe for preparing the UV-curable coatings is

17　given in **Table 1**. The reaction equations and schematic diagram of the synthesis route of the

18　coatings prepared with HBPUA oligomers and PETMP are illustrated in **Scheme 1c**.

19　**3.2. UV-curing behaviour**

20　For further theoretical exploration, the conversion rate of double-bond (C=C) and thiol groups was

21　investigated firstly due to the fact that the properties of the reactive components would have an

22　impact on the key properties of the resultant UV-curable films[21]. The UV-curing results were
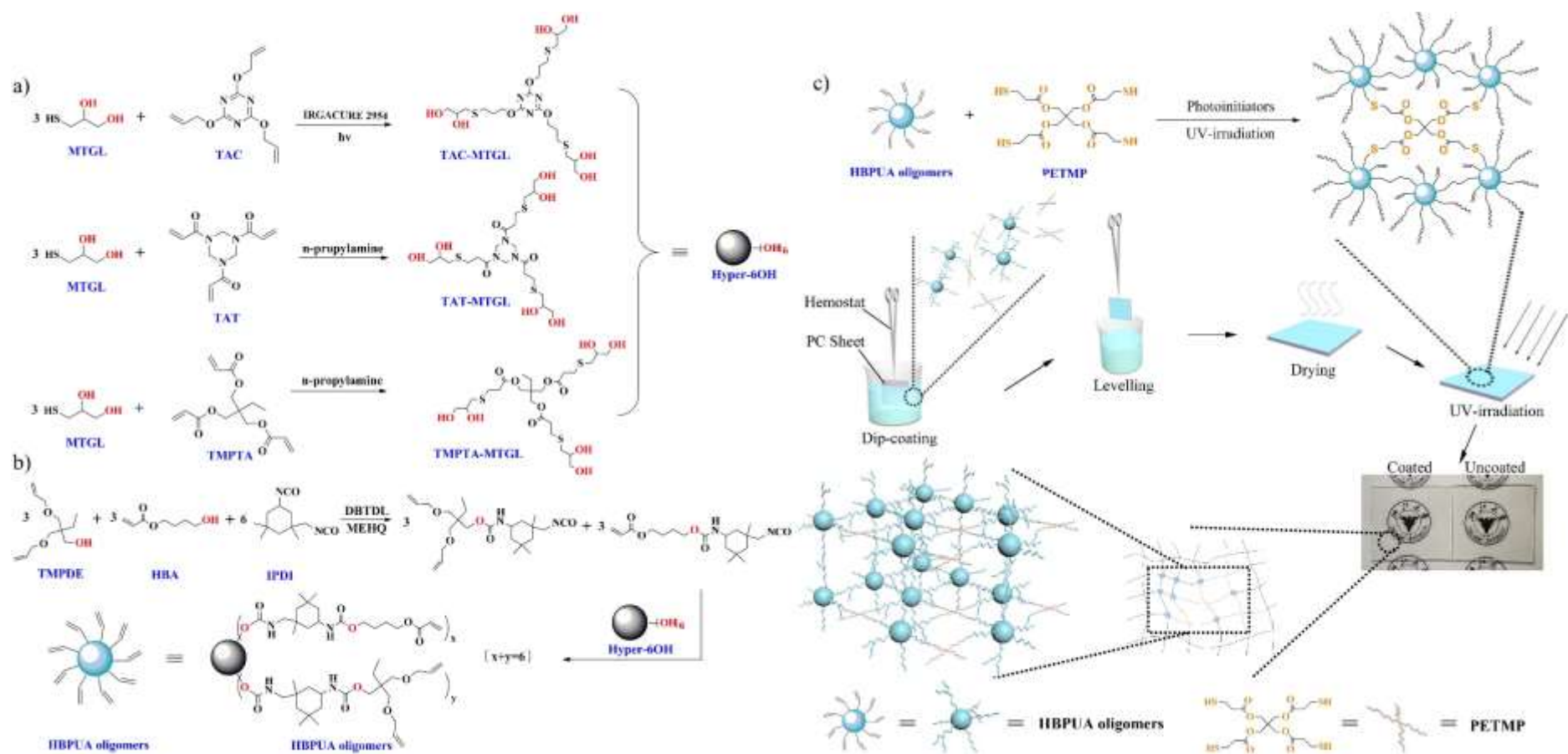
Scheme 1. Scheme of reactions to prepare a) Hyper-6OH and b) HBPUA oligomers. c) The reaction equations and schematic diagram for synthetic route of coatings

prepared with HBPUA oligomers and PETMP.

1 **Table 1** Detailed recipe for preparing the UV-curable coatings

Samples	Oligomers	PETMP	Irgacure 184	Irgacure TPO	IPA	Solid Content
	g	g	mg	mg	mL	wt%
S1	15.0021[a]	-	481.0	120.7	20	49.9
S1-1	12.0060[a]	2.9989	480.0	120.3	20	49.9
S2	15.0021[b]	-	480.9	120.5	20	49.9
S2-1	12.0050[b]	2.9990	481.0	120.3	20	49.9
S3	15.0010[c]	-	480.2	120.1	20	49.9
S3-1	12.0048[c]	3.0004	480.5	120.1	20	49.9
PUA-6	15.0080[d]	-	480.6	120.8	20	49.9

2 [a] HBPUA-TAC oligomers, [b] HBPUA-TAT oligomers, [c] HBPUA-TMPTA oligomers and [d] PUA-6 resin.

3 analysed by observing the intensity change of =C-H bending vibration at around 810 cm^{-1} (for

4 acrylate)[8] and 920 cm^{-1} (for allyl)[22] and thiol groups[22] at approximately 2560 cm^{-1}. In order to

5 eliminate the effect of scattering within the film, the characteristic absorption peaks of carbonyl

6 groups (C=O) at about 1725 cm^{-1} were used as the internal standard[8,23], as the intensity of the peak

7 (C=O) was hardly changed in the FT-IR spectra pre- and post-curing. The area of the absorption

8 peak was calculated by the integration function in the OMNIC 8.5 software. Thereby, the degree of

9 double bonds and thiols conversion was determined using eqn. (4) that follows (The former

10 coefficient is 1/3 and the latter is 2/3, since the mole ratio of C=C between acrylate and allyl groups

11 is 1:2.):[8,22]

12 $X = \left(\frac{1}{3} \times \frac{(A_{810}/A_{1725})_0 - (A_{810}/A_{1725})_t}{(A_{810}/A_{1725})_0} + \frac{2}{3} \times \frac{(A_{920}/A_{1725})_0 - (A_{920}/A_{1725})_t}{(A_{920}/A_{1725})_0}\right) \times 100$ (4a)

1     $Y = \left(\dfrac{(A_{2560}/A_{1725})_0 - (A_{2560}/A_{1725})_t}{(A_{2560}/A_{1725})_0} \right) \times 100$ (4b)

2   Where X and Y are the conversion rates of C=C and -SH groups. A_0 and A_t are the relative

3   absorptions of C=C and -SH pre- and post-UV irradiation, respectively.

4   As shown in **Figure 1**, for the coating without PETMP (neat HBPUA), the absorption peak of double

5   bonds still exists after exposure to UV irradiation, indicating that insufficient polymerisation occurs

6   within such coatings due to the fact that allylic double bonds are not very reactive in UV-induced

7   homopolymerization[24]. The detailed conversion rates of C=C and -SH are listed in **Table 2**, for

8   convenience of demonstrating the relationship between the curing behaviour of the films and the

9   molecular structure of the active components. From **Table 2**, as a comparison, it can be seen that

10   the C=C conversion rates of S1-1, S2-1 and S3-1 are 82.7%, 87.9% and 95.7%, respectively, which

11   are higher than those of S1 (38.5%), S2 (63.4%) and S3 (77.5%). Besides, it can be seen that -SH is

12   nearly all consumed after exposure to UV-radiation in the case of systems that contains PETMP.

13   The reason of the varying C=C conversion rate can be explained by the low reactivity of allyl groups

14   and the efficient thiol-ene click reaction after the addition of PETMP[19], respectively.

15   From another point of view, the C=C conversion of all samples can be ranked by the order of S1 <

16   S2 < S3 and S1-1 < S2-1 < S3-1 under the same type, showing that S1 and S1-1 have the lowest

17   C=C conversion rate and S3 and S3-1 had the highest rate of conversion. It is well known that in

18   free radical photo-polymerisation reactions, the auto-acceleration phenomenon can be observed,

19   through the rapid increase of polymerisation rate despite the high viscosity of UV-curing systems[25].

20   The more the flexible polymer chain and the lower coating solution, the more vigorous the auto-

21   acceleration effect that results in the high C=C conversion rate[26]. Therefore, the viscosities of

22   prepared coating solutions were measured. As shown in **Figure 1d**, the viscosities of S1 series
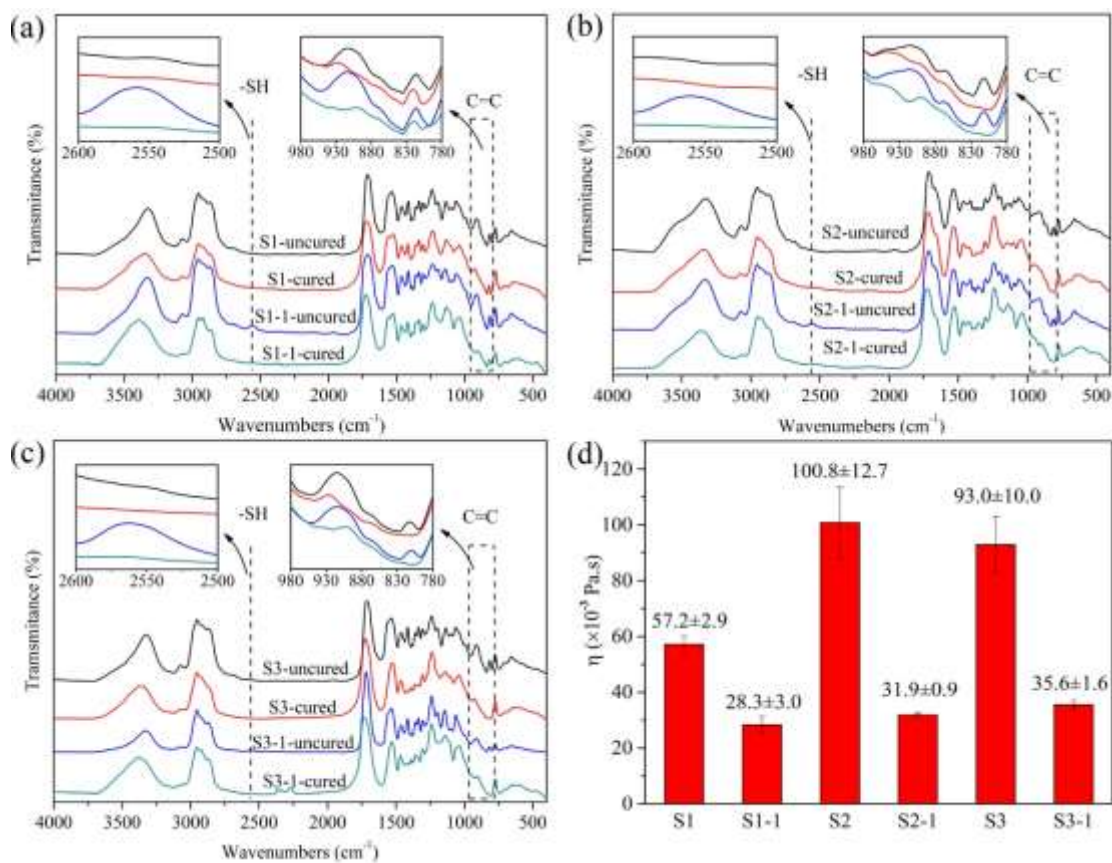
Figure 1. FT-IR spectra of the films prepared with a) HBPUA-TAC, b) HBPUA-TAT and c) HBPUA-TMPTA oligomers before and after being UV-cured, respectively. d) The viscosity of prepared coating solutions at 25 °C.

Table 2 The detailed conversions of C=C and -SH in the coatings prepared with HBPUA oligomers.

Coatings	S1	S1-1	S2	S2-1	S3	S3-1
C=C (%)	38.5	82.7	63.4	87.9	77.5	95.7
-SH (%)	-	98.6	-	100	-	100

(S1 and S1-1) are 57.2±2.9 mPa·s and 28.3±3.0 mPa·s, which are lower than S2 series (S2: 100.8± 12.7 mPa·s and S2-1: 31.9±0.9 mPa·s) and S3 series (S3: 93.0±10.0 mPa·s and S3-1: 35.6±1.6 mPa·s). This is because the molecule weight of HBPUA-TAT and HBPUA-TMPTA oligomers is higher than HBPUA-TAC oligomers. Additionally, the analysis of viscosity means that coatings of S1 series should have the highest conversion owing to their lowest viscosity of coating solutions.

1   Conversely, coatings of S1 series possess the lowest C=C conversion rate. Considering the

2   distinction of hyperbranched cores, the reason of different C=C conversion rates could be attributed

3   to the rigidity of hyperbranched cores. The triazine rings (S1 and S1-1) constrained the chain motion

4   during UV-curing owing to its rigidity as opposed to those cores (S3 and S3-1) having flexible

5   chains[27]. Because of their modest rigidity, the hyperbranched cores in S2 and S2-1 led to the medium

6   conversion rate of double bonds among all prepared HBPUA coatings.

7   **3.3. Analysis of physical properties**

8   In this study, in order to further ascertain the consistency of the double bond conversion and the

9   chemical crosslinking, the gel content of films prepared with HBPUA oligomers (HBPUA coatings)

10   was assessed with the aid of Soxhlet extraction. As shown in **Figure 2a**, the gel content of coatings

11   based on PETMP increases up to 95 wt.% compared with neat HBPUA coatings, and the order of

12   gel content follows the order S1 series < S2 series < S3 series, both of these observations are

13   consistent with the profile of the rate of double bond conversion. In other words, the degree of

14   chemical crosslink of all samples follows the order of the rate of double bond conversion. Besides,

15   the S1 coating has a high gel content of 92.3±0.4 wt.% in spite of the relatively lower double bond

16   conversion rate at 38.5%. It is considered that this is due to high functionality of oligomers. Thus,

17   if only one of the terminal C=C groups in oligomers attached to the polymer matrix via

18   polymerisation, the resulting modified oligomers would not be soluble in acetone used for the

19   Soxhlet extraction, which resulted in the high gel content despite the low consumption of double

20   bonds.

21   Additionally, the swelling properties of prepared coatings in acetone were measured shown in

22   **Figure 2b**, for the purpose of investigating the crosslinking density (total crosslinking including

1 physical and chemical crosslinking) of coatings[28,29]. The results reveal that the swelling ratio of

2 coatings is low (less than 50%) because of highly crosslink, and is ranked by the order S1 series >

3 S2 series > S3 series, revealing that the S1 series has the lowest crosslink density but the S3 series

4 possesses the highest crosslink density, indicating the consistency of chemical crosslinking and total

5 crosslinking. The reason could be ascribed to the similar composition and structure of three HBPUA

6 oligomers that generate similar intermolecular interaction and chain entanglement, resulting in the

7 similar physical crosslinking of prepared coatings in this study. Furthermore, the total crosslink

8 density of coatings is increased after the introduction of PETMP. The water absorption of the UV-

9 cured coating was reduced upon the introduction of thiol groups (**Figure 2c**), which can be

10 interpreted by the increase of crosslinking, since the more compact network would result in smaller

11 porous volume[30]. Nevertheless, despite its relatively low crosslink density, the S1-1 coating exhibits
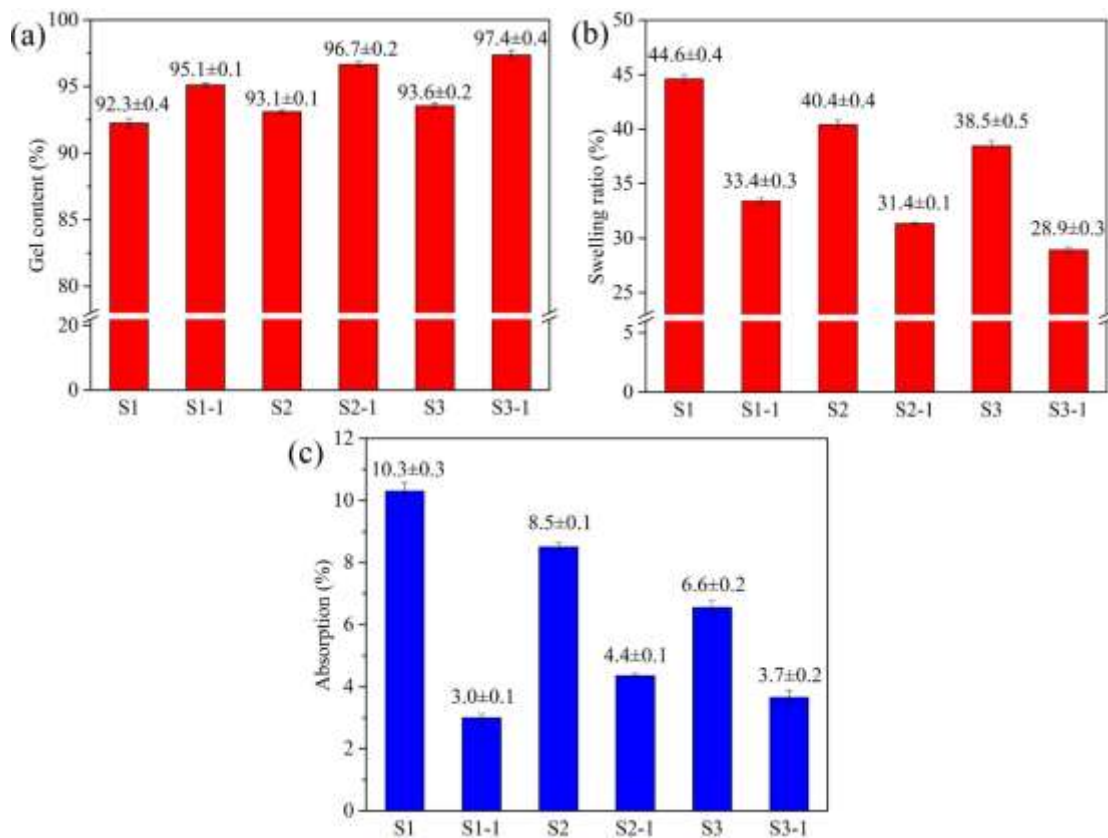
13 **Figure 2.** a) Gel content, b) swelling ratio and c) water absorption of the prepared HBPUA coatings.

1   the lowest water absorption compared with S2-1 and S3-1 films, demonstrating another impact

2   factor of water absorption that the triazine rings (S1-1) have the highest hydrophobicity within the

3   diverse hyperbranched cores in the present study.

4   **3.4. Dynamic mechanical analysis**

5   The degree of crosslinking, rigidity and crystallinity *etc*. affect the viscoelastic property of UV-cured

6   films[31]. To study the structure-property relationship in reference to the hyperbranched cores

7   concerned, DMA technique was employed to investigate the thermal mechanical property of all of

8   the prepared films. The glass transition temperature (T_g) is defined as the peak of tan δ curve. The

9   crosslink density (v_e) is calculated from the formula: $v_e = E'_{rubb}/3RT$, where E'_{rubb} is the storage

10   modulus in the rubbery plateau region, R is the gas constant and T is temperature in Kelvin where

11   rubbery plateau region emerges[27]. It is well-known that higher rigidity of chain segments and

12   crosslink density of networks result in higher T_g and the inclusion of flexible chains leads to lower

13   T_g value[32].

14   As shown in **Figure 3** and **Table 3**, the T_g of pure HBPUA coatings (S1, S2 and S3) are higher than

15   those of coatings containing PETMP (S1-1, S2-1 and S3-1), indicating that the addition of PETMP

16   causes a reduction in T_g. Whereas, the rising trend of the storage modulus (E'_{rubb}) in the rubbery

17   plateau region emerging from around 80-110 °C was observed when PETMP was introduced,

18   revealing an enhancement in the crosslink density v_e (**Table 3**). Furthermore, the magnitude of tan

19   δ value can be utilised as an assessment of the damping property of materials[31]. The lower tan δ

20   peak values (tan δ_{max}) are observed in the films containing PETMP (**Table 3**), disclosing an evidence

21   to the decrease in the physical crosslink density, since the tan δ_{max} value reflects the degree of

22   intermolecular friction mainly caused by the physical crosslinking. Thereby, we arrived at a

1   conclusion about the contradictory phenomena between the increase of crosslink density and the

2   decrease of T_g from the above finding, that such phenomena was due to the occurrence of the

3   increased internal plasticisation of flexible thioether and the decreased intermolecular forces of
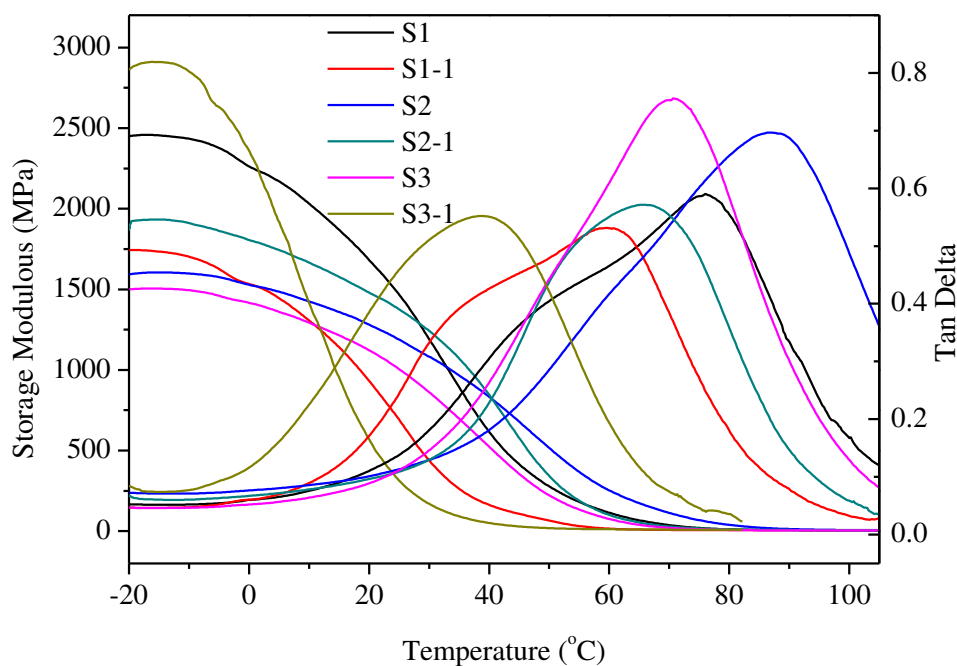
4

5   **Figure 3.** Lost factor (tan δ) curves of UV-curable films as a function of temperature.

6   **Table 3** Dynamic mechanical properties of the UV-cured coatings.

| Samples	tan δ_{max}	E'_{rubb}(MPa)	T_g(°C)	v_e(mmol/cm^3)
S1	0.59	5.11	76	0.55[a]
S1-1	0.53	6.39	60	0.73[b]
S2	0.70	5.52	87	0.61[c]
S2-1	0.57	7.06	66	0.8[a]
S3	0.75	6.26	71	0.67[a]
S3-1	0.55	9.30	39	1.06[b]

7   [a] T is 373.15 K. [b] T is 353.15 K. [c] T is 380.15 K.

1 hydrogen bonding (urethane groups) when PETMP was added[33], therefore reducing the T_g.

2 Interestingly, although the S3 series films possess the highest crosslink density compared with the

3 S1 and S2 series, the T_g values of these coatings are lowest (**Table 3**), proving that with regard to

4 the influence on the rigidity of UV-curable coatings, the distinct rigidity of cores in the prepared

5 oligomers plays a more significant role than the degree of crosslinking. In other words, the rigid

6 core can endow coatings with high rigidity. As mentioned above, the higher rigidity results in the

7 higher T_g by constraining chain motion. Owing to their rigid cores, the S1 and S2 series films show

8 higher T_g than the S3 series, especially for the S2 series that have the highest T_g (87 °C for S2 and

9 66 °C for S2-1) among the same type of films because of the dual effect of the high crosslink density

10 and the modest rigidity of the hyperbranched cores[32].

11 **3.5. Analysis of mechanical properties**

12 The mechanical properties of the prepared films were examined via tensile testing and evaluated

13 according to the Yang's modulus (E), the tensile strength (σ) and the elongation at break (ε)[34]. As

14 shown in **Figure 4** and **Table 4**, the films without the addition of PETMP possess greater tensile

15 strength but smaller elongation at break than those coatings with added PETMP. The changes in the

16 tensile strength could be attributed to the fact that the internal plasticisation of flexible thioether and

17 decreased intermolecular forces of hydrogen bonding resulted from the addition of PETMP, which

18 has been demonstrated by the previous DMA analysis. In spite of the neat HBPUA coatings showing

19 high tensile strength with low chemical crosslinking, they show their brittle property at around 6%

20 strain (**Table 4**). The relatively easy break of the physical crosslinking in such films occurred when

21 stress was increased to certain values (around 8.5 MPa), causing that the insufficient amount of

22 covalent bonds inside such polymers resisted the force directly, which results in brittleness of the

1 films. The introduction of PETMP into the HBPUA resins is equivalent to reducing the

2 concentration of hard segments (urethane groups) and increasing the content of soft segments

3 (flexible thioether chains) in the films[30], which is inferior to σ value but beneficial to ε value.

4 Therefore, the prepared coatings containing PETMP exhibit superior toughness reaching 43% strain
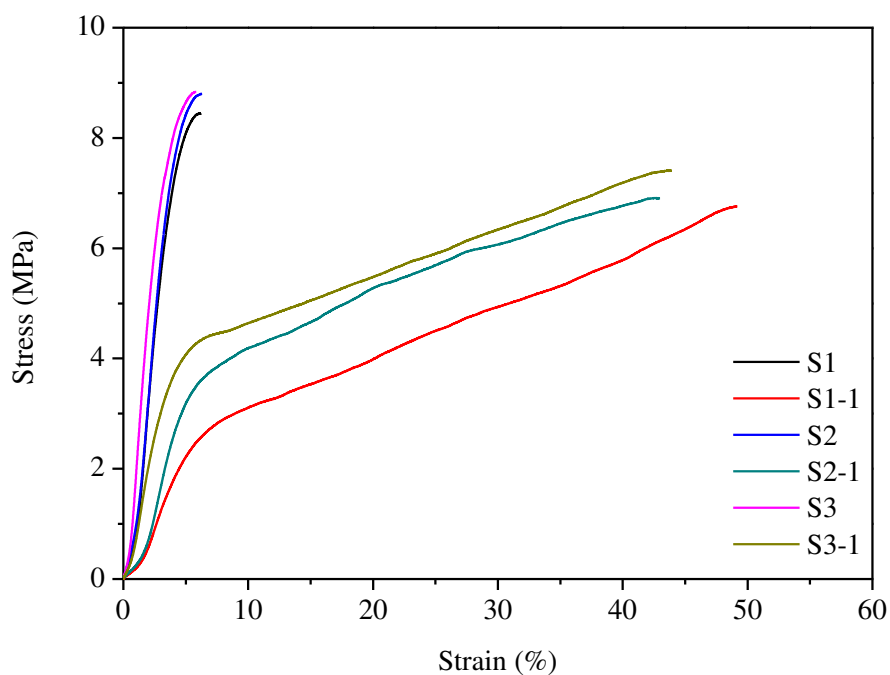
5

6 **Figure 4.** Tensile stress vs strain curves of the UV-cured films prepared with HBPUA oligomers.

7 **Table 4** Mechanical properties in the UV-cured HBPUA films.

Samples	E (MPa)	σ (MPa)	ε (%)
S1	236	8.44	6.2
S1-1	67	6.76	49.2
S2	275	8.80	6.3
S2-1	105	6.90	43.0
S3	277	8.84	5.8
S3-1	131	7.41	43.9

1   (**Table 4**), which is consistent with the analysis of flexibility mentioned earlier in this paper.

2   Moreover, Yang's modulus of the films dramatically reduces after the addition of PETMP (**Table 4**),

3   exhibiting the same changed tendency to the tensile strength. For the films containing PETMP, they

4   follows the order of S3-1>S2-1>S1-1 in the tensile strength, revealing that the higher degree of

5   crosslinking will obtain outstanding mechanical performance. Overall consideration, the S1-1 film

6   achieves the best mechanical property among all samples with 6.76 Mpa in σ and 49.2% strain in ε

7   (**Table 4**). In short, although the main factor in influencing the mechanical performance is crosslink

8   degree, the rigidity of the hyperbranched core can also affect the crosslink density of the coatings,

9   further changing the mechanical property of the coatings.

10   **3.6. Analysis of thermal properties**

11   The thermogravimetric analysis (TGA) of the prepared UV-cured coatings under N_2 atmosphere

12   are shown in **Figure 5a**, including their corresponding derivative weight loss (DTG) curves (**Figure**

13   **5b**). The decomposition of the polyurethane acrylate films consisted of two phases as indicated by

14   the appearance of two main weight-loss regions with peak maxima around 310 °C and 420 °C in

15   the DTG curves, respectively. The weight-loss below 200 °C can be attributed to the removal of

16   solvent and moisture and the decomposition of micromolecule[35]. The first decomposition stage

17   corresponds to the breakage of urethane linkage (hard segments), and the soft segments decompose

18   at the second phase. Evidently, the phenomenon that the boundary between hard segments and soft

19   segments became obscure occurred in the DTG curves when PETMP was added (**Figure 5b**). This

20   could be explained by the fact that PETMP can interact with hard segments through its carbonyl

21   groups, subsequently promoting phase mixing. For the thermal stability, it is obvious that the

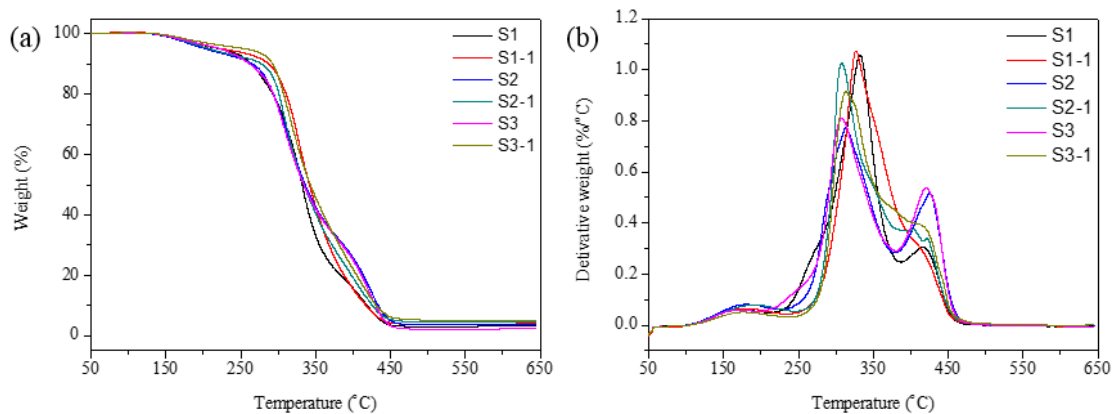22   coatings containing PETMP exhibit higher thermal stability than those coatings without thiol groups

Figure 5. TGA (a) and DTG (b) curves of the UV-cured films.

in the hard segments, but reverse trend in the soft segments. As explained, the addition of PETMP

simultaneously enhances the crosslink density and reduces the amount of urethane linkage which

promotes the thermal stability in the hard segments[36], and the increasing number of flexible chains

accounts for the inferior thermal stability of those films prepared based on PETMP in the soft

segments. This is not altogether unexpected for the reduction of thermal stability in the soft segments,

as the bond strength of C-S (272 kJ/mol) is much lower than that of C-C (346 kJ/mol)[37]. Moreover,

it is the expected consequence that the S1 coating shows poor thermal properties among all samples

in the soft segments due to its low crosslink density, since it could be easily decomposed into small

molecules because of its unreacted or partially reacted oligomers when the second decomposition

stage emerges. In a word, all samples show good thermal properties that the decomposition

temperature exceeds 150 °C.

3.7. Analysis of coating properties

The surface properties such as the pencil hardness, flexibility and adhesion of the prepared coatings

are of significant importance for application as protective film on PC cover for mobile phones

(**Figure 6a**). For the pencil hardness test, it can be seen that the coatings prepared with PETMP

possess higher pencil hardness than the neat HBPUA coatings, which is enhanced to more than 4H

1   from 1H owing to the enhancement in the degree of crosslink density (**Table 5**). Interestingly,

2   although the S1-1 coating obtains lowest crosslinking extent within the coatings prepared with

3   PETMP, it shows the highest hardness 5H, which is expected to observe because of the existence of

4   the rigid triazine core. That can be ascribed to the fact that in terms of increasing rigidity, the rigid

5   core is more remarkable than the crosslink density of coatings (S1-1, S2-1 and S3-1) in the present

6   research, which has been discussed in the DMA section. The more flexible chain resulted from the

7   hyperbranched core would easily generate chain motion upon load, leading to the reduction of the

8   amounts of the covalent bond used to withstand force in the stressed region, thereby such coatings

9   exhibit the inferior pencil hardness. As shown in **Table 5**, the flexibility and adhesion of the coating

10   based on pure HBPUA resins are dramatically improved with the addition of PETMP from 12 mm

11   to less than 2 mm and from 5 up to 1, respectively. The reason of increased toughness could be

12   attributed to the increment of flexible thioether chains and the reduction of hydrogen bonding, which

13   reveals the same trend as elongation at break. The influences of resins on the adhesion of coatings

14   can be summarized in several aspects, such as hydrogen bonding with substrates and the flexibility

15   *etc*[38]. The prominent enhancement in flexibility mainly accounts for the increment of adhesion.

16   **Table 5** Mechanical properties in the UV-cured HBPUA films.

Samples	S1	S1-1	S2	S2-1	S3	S3-1	PUA-6
Pencil Hardness	1H	5H	2H	5H	2H	4H	4H
Flexibility (mm)	12	< 2	12	< 2	12	<2	<2
Adhesion	0B	5B	0B	4B	0B	4B	5B

17   In order to comprehend profoundly the difference in the neat PC sheet and PC sheet coated with the

18   S1-1 resin and commercial PUA resin, the optical pictures are exhibited in **Figure 6**. It is clear to

1 observe that there is no dramatic difference in the transparency, and both of the S1-1 coating and

2 the PUA-6 coating achieved good adhesion level of 0. The pencil hardness test was implemented

3 by the 6H pencil according to ASTM D 3363. As shown in **Figure 6**, the surface of the uncoated PC

4 sheet is severely scratched because of its low intrinsic surface hardness. However, the surface

5 hardness can be prominently enhanced after coating, particularly for the S1-1 coating that the scratch

6 in surface is barely visible. Thus, we can conclude that S1-1 resin displays the superior surface

7 property than the commercial PUA resin, which has potential to be applied as protective film of PC

8 cover and protect PC surface well.
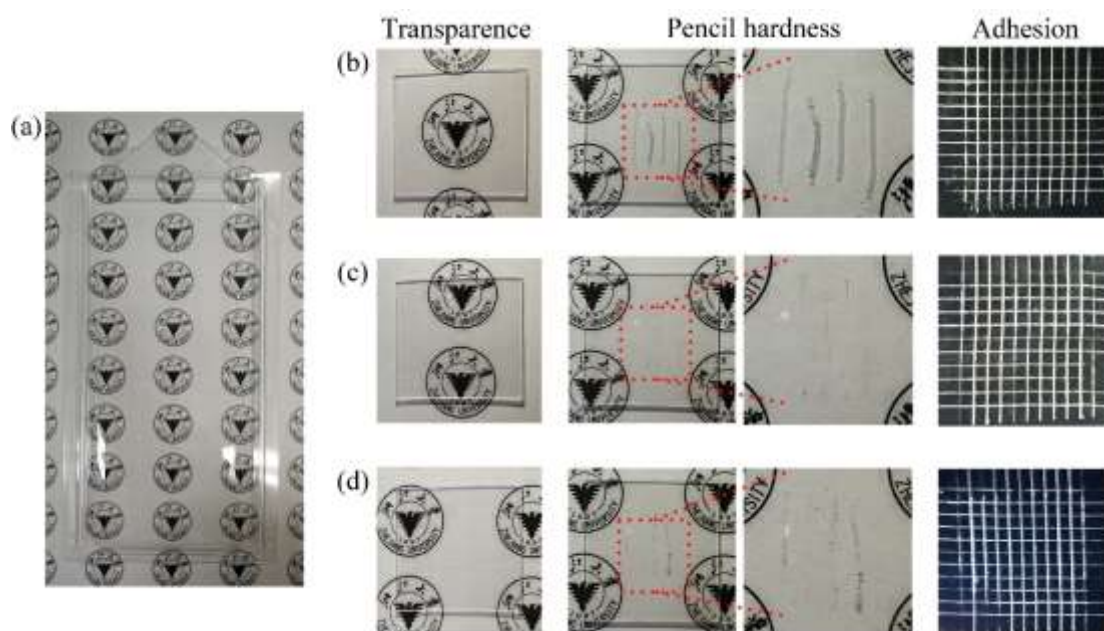
9

10 **Figure 6.** a) A whole PC sheet of phone cover. The difference in transparency, pencil hardness and

11 adhesion among b) uncoated PC sheet, PC sheet coated with c) S1-1 and d) PUA-6.

12 **Conclusion**

13 In the research reported in this paper, three different polyurethane acrylate oligomers containing

14 diverse hyperbranched cores were successfully synthesised and characterised by ^{1}H NMR and GPC.

15 For the purpose of promoting the double bond conversion, certain amounts of PETMP were each

blended into the pure HBPUA resin to form UV-curable resins. Then, a series of performance

coatings were prepared by dip-coating followed by UV-irradiation. From the FT-IR results obtained,

it is seen that the double bond conversion follows the order of S1 series < S2 series < S3 series due

to the decreasing rigidity of the hyperbranched cores, and the gel content reveals the consistency of

the double bond conversion and the chemical crosslink density. PETMP plays a significant role in

influencing the property of coatings owing to its internal plasticisation effect and the rapid 'click'

reaction. The DMA results reveal that the total crosslink density of the films containing the same

hyperbranched core increases after the introduction of thiol groups, and the rigid core is more

influential than the crosslink density with regard to increasing rigidity in the present research. The

S1-1 coating displays superior pencil hardness, adhesion and mechanical property among all

coatings reaching 5H, 0 and 6.76 MPa in tensile strength and 49.2% strain in elongation, respectively.

Compared to the commercially available resin that gives a pencil hardness of 4H, the prepared

coatings have a higher pencil hardness. All samples exhibit good thermal property giving high

decomposition temperature. Thus, it would appear that the coating prepared exhibits a potential for

application in protecting PC cover of mobile phones.

References

1 Chang, C. C., Oyang, T. Y., Hwang, F. H., Chen, C. C. & Cheng, L. P. Preparation of

   polymer/silica hybrid hard coatings with enhanced hydrophobicity on plastic substrates.

1   *Journal of Non-Crystalline Solids* **358**, 72-76 (2012).

2 2 Medda, S. K. & De, G. Inorganic-organic nanocomposite based hard coatings on plastics

3   using in situ generated nano-SiO₂ bonded with □Si-O-Si□PEO hybrid network. *Industrial*

4   *& Engineering Chemistry Research* **48**, 4326-4333 (2009).

5 3 Nakayama, N. & Hayashi, T. Synthesis of novel UV-curable difunctional thiourethane

6   methacrylate and studies on organic-inorganic nanocomposite hard coatings for high

7   refractive index plastic lenses. *Progress in Organic Coatings* **62**, 274-284 (2008).

8 4 Xu, J., Pang, W. & Shi, W. Synthesis of UV-curable organic-inorganic hybrid urethane

9   acrylates and properties of cured films. *Thin Solid Films* **514**, 69-75 (2006).

10 5 Hwang, D. K., Moon, J. H. & Shul, Y. G. Scratch resistant and transparent UV-protective

11   coating on polycarbonate. *Journal of Sol-Gel Science and Technology* **26**, 783-787 (2003).

12 6 Branko, D. Synthesis of new hyperbranched urethane-acrylates and their evaluation in UV-

13   curable coatings. *Progress in Organic Coatings* **51**, 320-327 (2004).

14 7 Mishra, R. S., Mishra, A. K. & Raju, K. V. S. N. Synthesis and property study of UV-curable

15   hyperbranched polyurethane acrylate/ZnO hybrid coatings. *European Polymer Journal* **45**,

16   960-966 (2009).

17 8 Yin, W., Zeng, X., Li, H., Hou, Y. & Gao, Q. Synthesis, photopolymerization kinetics, and

18   thermal properties of UV-curable waterborne hyperbranched polyurethane acrylate

19   dispersions. *Journal of Coatings Technology & Research* **8**, 577 (2011).

20 9 Lv, C., Hu, L., Yang, Y., Li, H., Huang, C. & Liu, X. Waterborne UV-curable polyurethane

21   acrylate/silica nanocomposites for thermochromic coatings. *RSC Advances* **5**, 25730-25737

22   (2015).

10   Li, K., Shen, Y., Fei, G., Wang, H. & Chen, W. The effect of PETA/PETTA composite system on the performance of UV curable waterborne polyurethane acrylate. *Journal of Applied Polymer Science* **132**, 41262 (2015).

11   Park, J. M. *et al.* Synthesis and properties of UV-curable polyurethane acrylates containing fluorinated acrylic monomer/vinyltrimethoxysilane. *Polymer Bulletin* **72**, 1921-1936 (2015).

12   Mishra, V., Desai, J. & Patel, K. I. High-performance waterborne UV-curable polyurethane dispersion based on thiol–acrylate/thiol–epoxy hybrid networks. *Journal of Coatings Technology & Research* **14**, 1-13 (2017).

13   Zhang, J., Xu, H., Hu, L., Yang, Y., Li, H., Huang, C. & Liu, X. Novel waterborne UV-curable hyperbranched polyurethane acrylate/silica with good printability and rheological properties applicable to flexographic ink. *ACS Omega* **2**, 7546-7558 (2017).

14   Ren, L., Zhu, J., Liu, X., Zhen, W. & Yan, J. UV-curable coatings from multiarmed cardanol-based acrylate oligomers. *ACS Sustainable Chemistry & Engineering* **3**, 1313-1320 (2015).

15   Nam, K. H., Seo, K., Seo, J., Khan, S. B. & Han, H. Ultraviolet-curable polyurethane acrylate nanocomposite coatings based on surface-modified calcium carbonate. *Progress in Organic Coatings* **85**, 22-30 (2015).

16   Killops, K. L., Campos, L. M. & Hawker, C. J. Robust, efficient, and orthogonal synthesis of dendrimers via thiol-ene "Click" chemistry. *Journal of the American Chemical Society* **130**, 5062-5064 (2008).

17   Rim, C., Lahey, L. J., Patel, V. G., Zhang, H. & Son, D. Y. Thiol-ene reactions of 1,3,5-

triacryloylhexahydro-1,3,5-triazine (TAT): facile access to functional tripodal thioethers. *Tetrahedron Letters* **50**, 745-747 (2009).

18   Dzunuzovic, Tasic, Bozic, Babic & Dunjic. UV-curable hyperbranched urethane acrylate oligomers containing soybean fatty acids. *Progress in Organic Coatings* **52**, 136-143 (2005).

19   Yang, Z., Wicks, D. A., Hoyle, C. E., Pu, H., Yuan, J., Wang, D. & Liu, Y. Newly UV-curable polyurethane coatings prepared by multifunctional thiol- and ene-terminated polyurethane aqueous dispersions mixtures: Preparation and characterization. *Polymer* **50**, 1717-1722 (2009).

20   Lomölder, R., Plogmann, F. & Speier, P. Selectivity of isophorone diisocyanate in the urethane reaction influence of temperature, catalysis, and reaction partners. *Journal of Coatings Technology* **69**, 51-57 (1997).

21   Andrzejewska, E. & Andrzejewski, M. Sulfur-containing polyacrylates. IV. The effect of -S- linkages and -O- linkages on the photo- and thermally induced polymerization of dimethacrylates. *Journal of Polymer Science Part a-Polymer Chemistry* **31**, 2365-2371 (1993).

22   Yang, Z., Wicks, D. A., Yuan, J., Pu, H. & Liu, Y. Newly UV-curable polyurethane coatings prepared by multifunctional thiol- and ene-terminated polyurethane aqueous dispersions: Photopolymerization properties. *Polymer* **51**, 1572-1577 (2010).

23   Wu, J., Ma, G., Li, P., Ling, L. & Wang, B. Surface modification of nanosilica with acrylsilane-containing tertiary amine structure and their effect on the properties of UV-curable coating. *Journal of Coatings Technology and Research* **11**, 387-395 (2014).

24   Hoyle, C. E., Lee, T. Y. & Roper, T. Thiol-enes: Chemistry of the past with promise for the future. *Journal of Polymer Science Part a-Polymer Chemistry* **42**, 5301-5338 (2004).

25   Asif, A., Shi, W. F., Shen, X. F. & Nie, K. M. Physical and thermal properties of UV curable waterborne polyurethane dispersions incorporating hyperbranched aliphatic polyester of varying generation number. *Polymer* **46**, 11066-11078 (2005).

26   Wu, J., Ma, G., Ping, L., Ling, L. & Wang, B. Surface modification of nanosilica with acrylsilane-containing tertiary amine structure and their effect on the properties of UV-curable coating. *Journal of Coatings Technology & Research* **11**, 387-395 (2014).

27   Zhang, Y., Asif, A. & Shi, W. Highly branched polyurethane acrylates and their waterborne UV curing coating. *Progress in Organic Coatings* **71**, 295-301 (2011).

28   Lucht, L. M. & Peppas, N. A. Macromolecular structure of coals: 2. Molecular weight between crosslinks from pyridine swelling experiments. Fuel **66**, 803-809 (1987).

29   Xie, H. Cheng, CY. Deng, XY. Fan, CJ. Du, L. Yang, KK. & Wang, YZ. Creating poly(tetramethylene oxide) glycol-based networks with tunable two-way shape memory effects via temperature-switched netpoints. *Macromolecules* **50**, 5155-5164 (2017).

30   Zhang, T., Wu, W., Wang, X. & Mu, Y. Effect of average functionality on properties of UV-curable waterborne polyurethane-acrylate. *Progress in Organic Coatings* **68**, 201-207 (2010).

31   Bao, F. & Shi, W. Synthesis and properties of hyperbranched polyurethane acrylate used for UV curing coatings. *Progress in Organic Coatings* **68**, 334-339 (2010).

32   Yu, Y., Liao, B., Li, G., Jiang, S. & Sun, F. Synthesis and properties of photosensitive silicone-containing polyurethane acrylate for leather finishing agent. *Industrial &*

Engineering Chemistry Research **53**, 564-571 (2014).

33   Otts, D. B., Heidenreich, E. & Urban, M. W. Novel waterborne UV-crosslinkable thiol-ene polyurethane dispersions: Synthesis and film formation. *Polymer* **46**, 8162-8168 (2005).

34   Hwang, H. D. & Kim, H. J. Enhanced thermal and surface properties of waterborne UV-curable polycarbonate-based polyurethane (meth)acrylate dispersion by incorporation of polydimethylsiloxane. *Reactive & Functional Polymers* **71**, 655-665 (2011).

35   Zhang, Q., Huang, C., Wang, H., Hu, M., Li, H. & Liu, X. UV-curable coating crosslinked by a novel hyperbranched polyurethane acrylate with excellent mechanical properties and hardness. *Rsc Advances* **6**, 107942-107950 (2016).

36   Xu, J., Jiang, Y., Zhang, T., Dai, Y., Yang, D., Qiu, F., Yu, Z. & Yang, P. Synthesis of UV-curing waterborne polyurethane-acrylate coating and its photopolymerization kinetics using FT-IR and photo-DSC methods. *Progress in Organic Coatings* **122**, 10-18 (2018).

37   Liu, C. Li, T., Zhang, J., Chen, S., Xu, Z., Zhang, A. & Zhang, D. Preparation and properties of phosphorous-nitrogen containing UV-curable polymeric coatings based on thiol-ene click reaction. *Progress in Organic Coatings* **90**, 21-27 (2016).

38   Jiao, Z., Yang, Q., Wang, X. & Wang, C. UV-curable hyperbranched urethane acrylate oligomers modified with different fatty acids. *Polymer Bulletin* **74**, 5049-5063 (2017).